Power Quality Monitoring in a System with Distributed and Renewable Energy Sources

Andrzej Nowakowski, Aleksander Lisowiec and Zdzisław Kołodziejczyk
Tele-and Radio Research Institute
Poland

1. Introduction

The chapter deals with three issues concerning power quality monitoring in power grids with distributed energy sources. The structure of the grid has been described with pointing out the sources of voltage disturbances and the disturbance susceptibility of the grid components. Conclusions have been drawn at what nodes it is necessary to employ power quality monitoring. The technical solutions needed to integrate power quality analysis functions into protection relay have been described. New types of voltage and current transducers for use in primary circuits of power station have been presented.

The growing share of unconventional energy sources in the total energy balance of distribution companies carries with itself a necessity to provide adequate energy quality and energy safety to the final user. The importance of this issue has been underlined by many documents accepted by the governments of the individual European countries and by the European Commission itself.

The successful integration of various energy sources and consumers in the grid with the general diagram presented in Figure 1 requires meeting the demands of energy sellers who want to sell electricity and consumers who want to use electricity in an economically efficient way. The grid has to be balanced and the energy supplied to the customer has to meet quality standards. The need to supply consumers with the required electricity carries with itself the necessity to monitor the power quality.

When incorporating renewable energy sources within power distribution networks it is very important to provide power quality analysis at many nodes in the network.

The nature of renewable energy sources is such that they produce either a DC voltage – as is the case with solar panels and energy containers in the form of supercapacitors or an AC voltage of varying frequency as is the case with wind turbines and wave turbines (Ackerman T. ed. 2005), (Gilbert M. 2004). The renewable energy sources must be either synchronized or converted to alternating current before their energy can be injected into the grid. The power electronic devices that convert AC voltage to DC voltage and DC voltage to AC voltage are inverters and during the conversion process disturbances in the form of harmonics, voltage sags and overshoots are created which have to be kept under control. Also many loads that are now connected to the power networks exhibit nonlinear dependence of drawn current on supply voltage. These nonlinearities are the source of higher current harmonics that are injected into the grid. As the impedance of the power

lines is not zero, voltage harmonics appear. Particularly important is the measurement and analysis of possible adverse effects of harmonics on the equipment connected to the network. Power quality analyzers that measure the harmonic content in the supply voltage are too expensive to apply at each node where the renewable source is connected to the network.
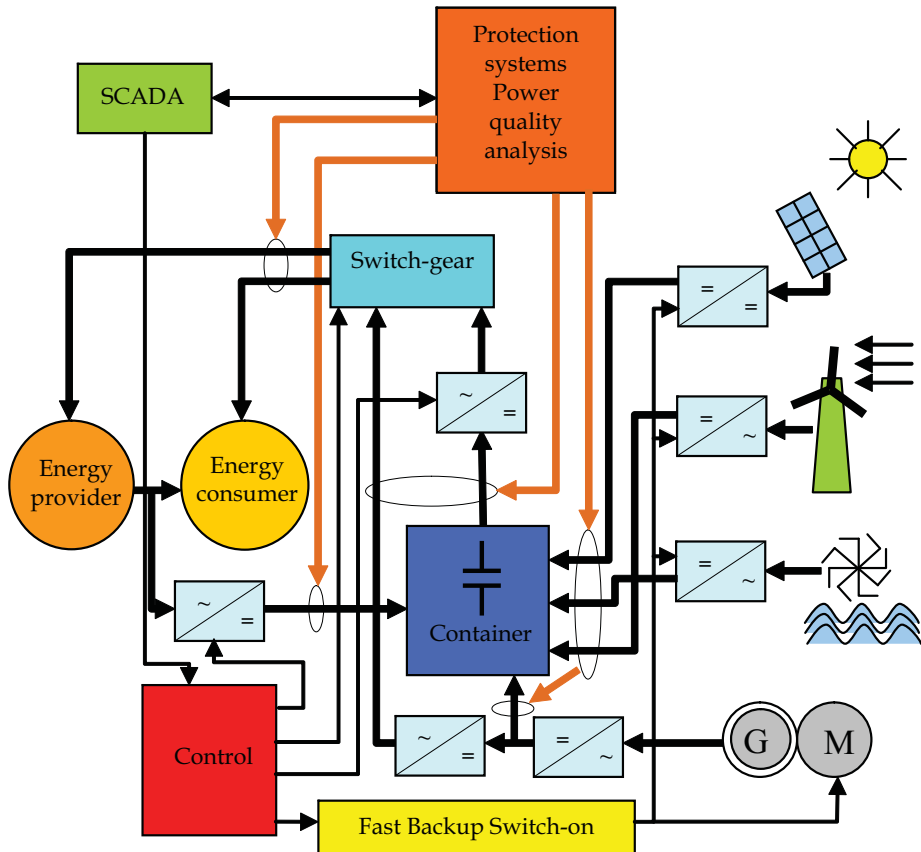

Fig. 1. A structure of protection, monitoring and control system integrating distributed renewable energy sources and energy containers

The solution to the problem of mass scale power quality monitoring and control is to equip conventional protection relays with power quality analysis functions, Figure 2. The natural nodes to place the combined devices are at the output of the inverters marked in Figure 2 by red color. The tremendous advance in the DSP microprocessor technology enables to implement the power quality analysis software, particularly harmonics and interharmonics level determination, at a very small additional cost for the end user. The advanced signal processing algorithms like signal resampling in the digital domain are the key to achieving design objectives. To keep the cost of the developed protection relay low, the developed algorithms should put minimal requirements on hardware.
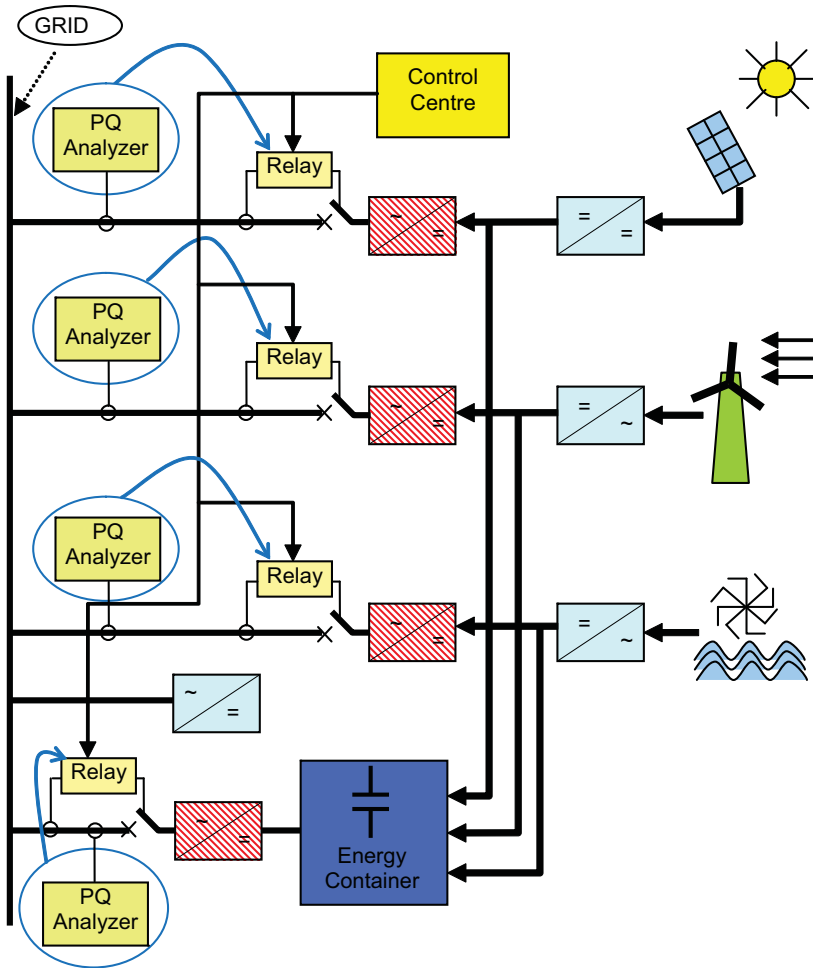
Fig. 2. Power grid with the nodes at which it is possible to combine protection functions with power quality analysis

2. Integrating power quality analysis and protection relay functions

The main issue in the development of protection relay integrated with power quality analyser is the necessity to elaborate efficient algorithms for line voltage and current signals frequency spectrum determination with harmonic and interharmonic content up to 2 kHz. The mass use of power quality monitoring, postulated in the previous paragraph, demands that incorporation of power quality analysis functions into protection relay comes at a negligible additional cost to the end user. The cost of the additional hardware has thus to be as low as possible with the burden of extra functionality placed on the software.

Modern microprocessor controlled protection relays employ sampling of analogue current and voltage signals and digital signal processing of the sample sequences to obtain signal

parameters like RMS, which are then used by protection algorithms. In this respect they are similar to stand alone power quality analysers that also carry out the calculations of signal parameters from sample sequences. The availability of fast and high resolution analogue to digital converters enables cost effective signal front end design suited equally well for protection relay and power quality analyser.
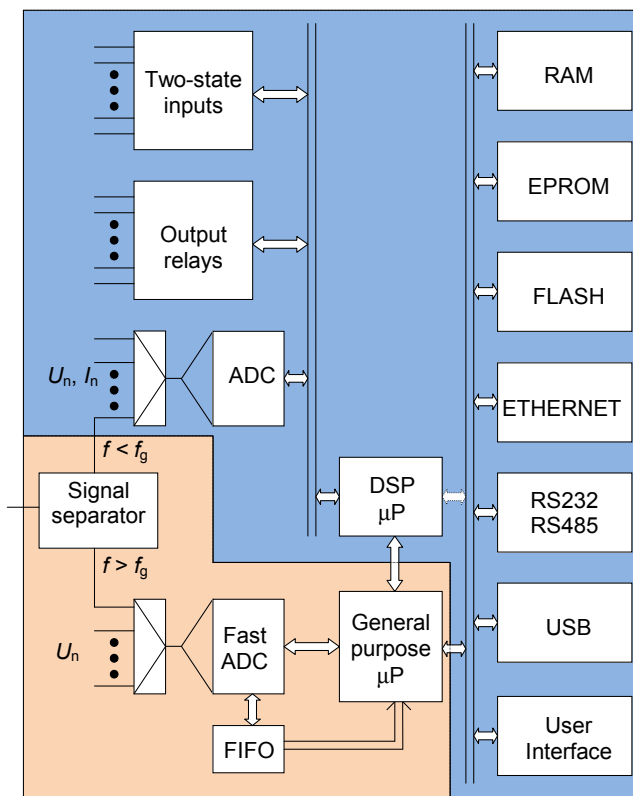

Fig. 3. Block diagram of combined protection relay and power quality analyser

The architecture of combined protection relay and power quality analyser has been shown in Figure 3. The architectures of power quality analyzer and protection relay are very similar. They differ only in the transient voltage surge measurement module, which has been marked by a different colour in Figure 3. While the basic signal parameterization software implemented in both devices uses Fourier techniques for spectrum determination, the protection relays contain additionally the protection algorithms software and power quality analyzers contain more elaborate spectrum analysis and statistical software. Power quality analyzers also have wider input bandwidth to measure accurately harmonic and interharmonic content of the signal up to 2 kHz. To merge protection relay and power quality analyser in a single device in a cost effective way it is necessary to employ advanced signal processing techniques like oversampling and changing the effective sampling rate in digital domain.

2.1 Harmonic and interharmonic content determination
2.1.1 Introduction

The international standards concerning power quality analysis (EN 50160, EN 61000-4-7:2002, EN 61000-4-30:2003) define precisely which parameters of line voltage and current signals are to be measured and the preferred methods of measurement in order to determine power quality. In compliance with these requirements, for harmonic content determination, power quality analyzers employ sampling procedures with sampling frequency precisely synchronized to the exact multiple of line frequency. This is necessary for correct spectrum determination as is known from Fourier theory (Oppenheim & Schafer, 1998). If the sampling frequency is not equal to the exact multiple of line frequency, the spectral components present in the signal are computed with error and moreover false components appear in the spectrum.

Efficient computation of signal spectrum with the use of FFT transform demands that the number of samples in the measurement interval be equal to the power of two. With sampling frequency synchronized to the multiple of line frequency, it is impossible to satisfy this requirement both in one line period measurement interval – when the measurement results are used for protection functions, and ten line periods measurement interval when interharmonic content is determined. This is the reason why some power quality analyzers available on the market offer interharmonic content measurement over 8 or 16 line periods interval. Another disadvantage of synchronizing sampling frequency to the line signal frequency is the inability to associate with each recorded signal waveform sample a precise moment in time. When the power quality meter is playing also the role of disturbance recorder, the determination of a precise time of an event is very difficult in such case. A better method to achieve the number of samples equal to the power of two both in one and ten line periods, with varying line frequency, is to use constant sampling frequency and employ digital multirate signal processing techniques.

As the digital multirate signal processing involves a change in the sample rate, the sampling frequency can be chosen with the aim of simplifying the antialiasing filters that precede the analog to digital converter. According to the EN 61000-4-7:2002 standard, the signal bandwidth that has to be accurately reproduced for power quality determination is 2 kHz. The complexity of the low-pass filter preceding the A/D converter depends significantly on the distance between the highest harmonic in the signal that has to be passed with negligible attenuation (in this case the 40-th harmonic) and the frequency equal to the half of the sampling frequency. When the sampling frequency around 16 kHz is chosen, a simple 3-pole RC active filter filters can be used.

2.1.2 Multirate digital signal processing in protection relay

In multirate digital signal processing (Oppenheim & Schafer, 1998) it is possible to change the sampling rate by a rational factor N/M using entirely digital methods. The input signal sampled with constant frequency f_s is first interpolated by a factor of N and then decimated by a factor of M – both these processes are called collectively resampling. The output sequence consists of samples representing the input signal sampled at an effective frequency f_{seff}, where

$$f_{seff} = f_s \cdot (N/M) \tag{1}$$

The first thing that has to be determined is how many samples are needed to calculate the spectral components of the signal. For protection purposes, the knowledge of harmonics up

to 11th used to be enough in the past. The increasing use of nonlinear loads (and competition) has led leading manufacturers of protection relays to develop devices with the ability to determine the signal spectrum up to 40 or even 50-th harmonic. Thus, taking into account that the number of samples, for computational reasons, must equal the power of two, 128 samples per period are needed (Oppenheim & Schafer, 1998). The ideal sampling frequency is then $f_{sid} = f_{line} \cdot 128$ Hz (= 6400 Hz at 50 Hz line frequency). For power quality analysis, the EN 61000-4-7 standard demands that the measurement interval should equal ten line periods and the harmonics up to 40th (equivalently interharmonics up to 400th) have to be calculated. This gives 1024 as the minimum number of samples over ten line periods meeting the condition of being equal to the power of two. The ideal sampling frequency f_{sid} for interharmonic content determination should be equal to $((f_{line})/10) \cdot 1024$ Hz which is 5120 Hz at f_{line} = 50 Hz. Knowing the needed effective sampling frequency and the actual sampling frequency f_s – which for the rest of the chapter is assumed to be equal to 16 kHz, the equation (1) can be used to determine interpolation and decimation N, M values. Tables 1 and 2 gather the values of N and M (without common factors) computed from (1) for a range of line frequencies.

f_{line}	49.5	49.55	49.6	49.65	49.7	49.75	49.8	49.85	49.9	49.95
N	99	991	248	993	497	199	249	997	499	999
M	250	2500	625	2500	1250	500	625	2500	1250	2500

Table 1. Interpolation and decimation factors protection function

50.0	50.05	50.1	50.15	50.2	50.25	50.3	50.35	50.4	50.45	50.5
2	1001	501	1003	251	201	503	1007	252	1009	101
5	2500	1250	2500	625	500	1250	2500	625	2500	250

Table 1, cont.

f_{line}	49.5	49.55	49.6	49.65	49.7	49.75	49.8	49.85	49.9	49.95
N	198	991	992	993	994	199	996	997	998	999
M	625	3125	3125	3125	3125	625	3125	3125	3125	3125

Table 2. Interpolation and decimation factors for interharmoncs determination

50.0	50.05	50.1	50.15	50.2	50.25	50.3	50.35	50.4	50.45	50.5
8	1001	1002	1003	1004	201	1006	1007	1008	1009	202
25	3125	3125	3125	3125	625	3125	3125	3125	3125	625

Table 2, cont.

For some line frequencies the values of N and M computed from (1) are very large, e.g. for f_{line} = 49.991 Hz, N = 49991 and M = 125000. The computational complexity of the resampling procedure depends on how large the values of N and M are.

The interpolation process consists in inserting a *N*-1 number of zero samples between each original signal sample pair. The resulting sample train corresponds to a signal with the bandwidth compressed with *N* ratio and multiplied on a frequency scale *N* times (Oppenheim & Schafer, 1998). To recover the original shape of the signal, the samples have to be passed through a low pass filter with the bandwidth equal to the *B/N* bandwidth of the signal prior to interpolation. In time domain the filter interpolates the zero samples that have been inserted between the original signal samples.
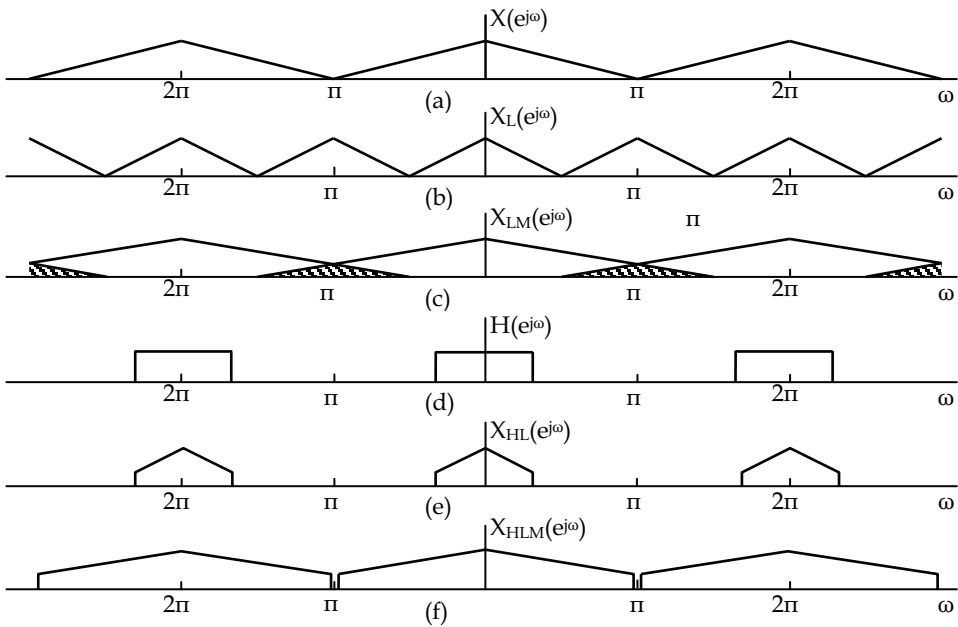
Fig. 4. The effect of interpolation and decimation on signal spectrum

The decimation process consists in deleting *M*-1 samples from each consecutive group of *M* samples. The resulting sample train corresponds to a signal prior to the decimation but with the bandwidth expanded by a factor of *M*. To prevent the effect of aliasing, the sample sequence to be decimated has to be passed through a low pass filter with the bandwidth equal to $2\pi/M$ in normalized frequency. The operation of interpolation and decimation on the bandwidth of the signal has been shown in Figure 4 for *N* = 2 and *M* = 3. In this figure $X(e^{j\omega})$ is the spectrum of the original signal, $X_L(e^{j\omega})$ is the spectrum of the original signal with zero samples inserted and $X_{LM}(e^{j\omega})$ the spectrum of the original signal with zero samples inserted and then decimated with the *M* ratio. As can be seen in Figure 4 c) there is a frequency aliasing. If the signal after interpolation is passed through a low pass filter with suitable frequency characteristic $H(e^{j\omega})$ the effect of frequency aliasing is avoided as shown in Figure 4 d).

To preserve as much of the bandwidth of the original signal as possible, the low pass filter used in the resampling process has to have a steep transition between a pass and stop bands. The complexity of the filter depends heavily on the magnitude of the greater of the values of *N* and *M*. This is one of the many reasons why the values of *N* and *M* should be

chosen as low as possible but at the same time the f_{eff} computed from (1) should be as close as is necessary to the ideal sampling frequency f_{sid}.

The accuracy with which f_{eff} is to approximate f_{sid} could be determined from simulating how different values of N and M affect the accuracy of spectrum determination. However some clues about the values of N and M can be obtained from EN 61000-4-7 standard. In chapter 4.4.1 it states that the time interval between the rising edge of the first sample in the measurement interval (200 ms in 50 Hz systems) and the rising edge of the first sample in the next measurement interval should equal 10 line periods with relative accuracy not worse than 0.03%. Therefore, for each line frequency, the values of N and M should be chosen so as the relative difference E_{eff} between the ideal sampling frequency f_{sid}, and the effective sampling frequency f_{eff} meets the following condition

$$E_{eff} = \left| \frac{\left(f_{seff} \cdot f_{sid} \right)}{f_{sid}} \right| \le 0.003 \tag{2}$$

The frequency characteristic of the low pass filter used in the resampling procedure depends on the values of N and M. If a different filter is used for each N, M pair it places a heavy burden on limited resources of DSP processor system in a protection relay. A solution to this problem is to fix the value of N and choose M according to the following formula

$$M = Round\left(\frac{N \cdot f_s}{\left(\frac{f_{line}}{L} \right) \cdot SN} \right) \tag{3}$$

where L is the number of periods used in the spectrum determination and SN is the number of the samples in L periods (128 samples per one period for protection functions, 1024 samples per 10 periods for power quality analysis). The $Round(x)$ function gives the integer closest to x. The low pass filter is then designed with the bandwidth equal to $2\pi/M_{min}$ where M_{min} is the value of M computed from (2) for highest line frequency f_{line}.

For power quality analysis when the interharmonics content has to be determined, N=600, the minimum value of M is 1630 at f_{line} = 57.5 Hz, the maximum value of M is 2206 at f_{line} = 42.5 Hz. The maximum absolute value of E_{eff} is equal to 0.03% and the effective sampling frequency is within the range recommended by EN 61000-4-7 standard. As the error of spectrum determination increases with increasing E_{eff} it is sufficient to carry out the analysis of the accuracy of spectrum determination for line frequency, for which the E_{eff} is largest. The obtained accuracy should then be compared with the accuracy of spectrum determination when the sampling frequency is synchronized to the multiple of the same line frequency with the error of 0.03%. For the analysis a signal composed of the fundamental component, 399 interharmonic with 0.1 amplitude relative to the fundamental, 400 interharmonic with 0.05 amplitude relative to the fundamental and 401 interharmonic with 0.02 amplitude relative to the fundamental should be selected. This is the worst case signal because on the one hand the error is greatest at the upper limit of the frequency range, and on the other hand when close interharmonics are present, there is leakage from the strongest interharmonic to the others. Figure 5 shows the spectrum of the test signal determined when the synchronization technique is used and Figure 6 shows the spectrum when the digital resampling technique is used. In both cases the resulting sample rate is identical.
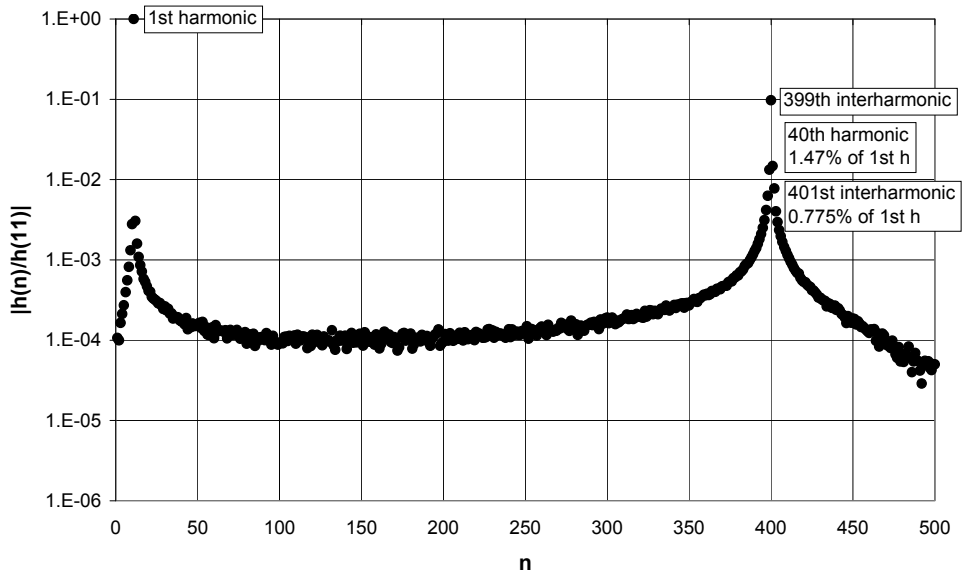
Fig. 5. Spectrum of the test signal when synchronization of the sampling frequency to the multiple of line frequency is used
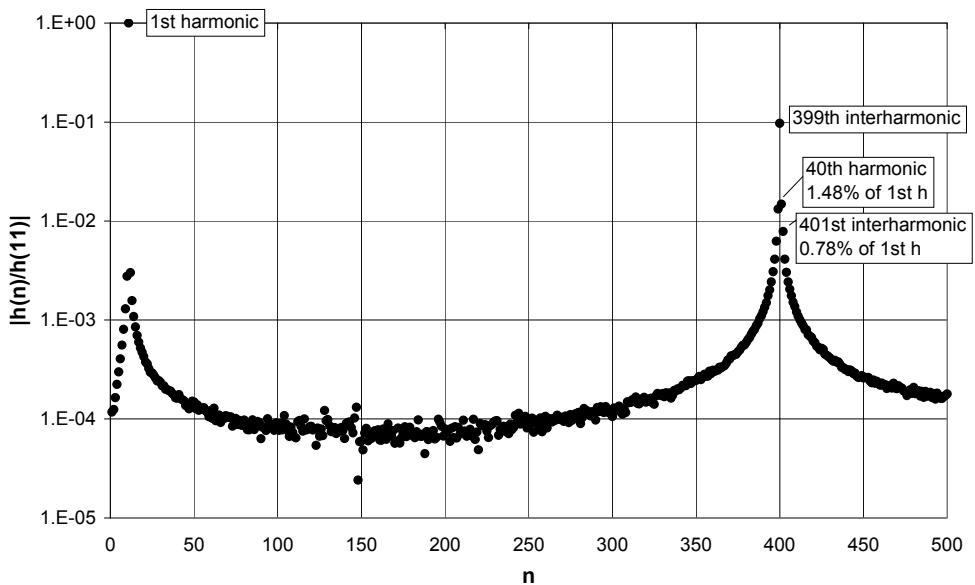
Fig. 6. Spectrum of the test signal when resampling technique is used

The two spectra are almost identical and they both give the same error in the interharmonic level determination. The level of 399th interharmonic is very close to the true value. However the level of 40th harmonic is almost three times higher than the true value and the level of 401st interharmonic is almost four times higher than the true value. The observed effect can be explained by leakage of the spectrum from 399th interharmonic of relatively large level to neighbouring interharmonics (Bollen & Gu 2006). The detailed analysis carried out for the whole range of line frequency and various signal composition shows that if the error between the ideal sample rate and actual sample rate at the input of Fourier spectrum computing procedure is the same, both methods give equally accurate results.

For the protection functions the needed frequency resolution is ten times lower than for interharmonic levels determination. It suggests, that the values of N and M can be chosen such that the maximum value of E_{eff} < 0.3%. With N=80, the minimum value of M equal to 174 at f_{line} = 57.5 Hz, and the maximum value of M equal to 235 at f_{line} = 42.5 Hz, the maximum absolute value of E_{eff} is equal to 0.284%. The detailed analysis shows that harmonics are determined with the accuracy which is better than 1%.

3. New input circuits used for parameters determination of line current and voltage signals

The measurement of line voltage and current signals for power quality analysis demands much higher accuracy than is needed for protection purposes. Traditional voltage and current transducers used in primary circuits of power stations cannot meet the requirements of increased accuracy and wide measurement bandwidth. New types of voltage and current transducers are needed with frequency measurement range equal to at least the 40-th harmonic of fundamental frequency, high dynamic range and very good linearity. For current measurements Rogowski coils may be used. They have been used for many years in applications requiring measurements of large current in wide frequency bandwidth. The traditional technologies used for making such coils were characterized by large man labour. Research work has been carried out at many laboratories to develop innovative technologies for Rogowski coil manufacture. These technologies are based on multilayer PCB.

3.1 Principle of PCB Rogowski coil construction

The principle of Rogowski coil operation is well known (http://www.axilane.com/PDF_Files/Rocoil_Pr7o.pdf). The basic design consists in winding a number of turns of a wire on a non-magnetic core, Figure 7.

The role of the core is only to support mechanically the windings. The voltage V(t) induced at the terminations is expressed by the following equation

$$V(t) = -\frac{d\Phi}{dt} = -\mu_0 \cdot n \cdot A \cdot \frac{dI}{dt} \tag{4}$$

where μ_0 is the magnetic permeability of the vacuum, n is the number of turns, A is the area of the single turn (referring to Figure 7, A=$\pi \cdot r^2$) and I is the current flowing in the conductor coming through the coil.
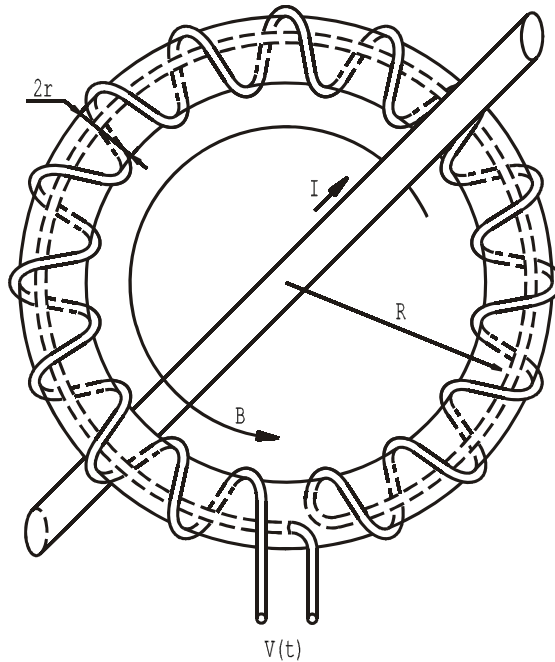
Fig. 7. A simplified construction of the Rogowski coil

The most important parameter of the Rogowski coil is its sensitivity *S*. It is the ratio of the RMS value of the voltage at coil terminations to the RMS value of the sine current flowing in the wire going through the centre of the coil. Because of the factor *dI/dt* in equation (4), the sensitivity is directly proportional to the frequency of the current signal. In applications of the Rogowski coil in the power industry sector the sensitivity is given at the fundamental line frequency 50 Hz or 60 Hz. The sensitivity of the coil which has the shape as shown in Figure 7, is given by the following formula:

$$S = \mu_0 \cdot A_{ef} \cdot \omega \cdot \frac{n}{2 \cdot \pi \cdot R} \tag{5}$$

where *n* is the total number of the turns, ω is the angular pulsation of the sinusoidal current I, and R is the radius of the coil. The factor *A* has been replaced with A_{ef} because in practice not every turn has to have the same dimensions. The last factor in the equation (5) shows that the sensitivity of the coil is directly proportional to the density *l* of the turns where $l = n/(2 \pi \cdot R)$. The PCB design of the Rogowski coil replaces the wire turns by induction coils printed on multilayer boards. On each layer there is a basic coil in the form of a spiral. The coils on neighboring layers are connected by vias. The vias can be buried or through. The buried vias leave more board space for the coil but are much more expensive to manufacture. A design of the first 4 layers of 16-layer board with buried vias is presented in Figure 8. Photos of the multilayer board designs with through and buried vias are presented in Figures 9 a) and 9 b) respectively.
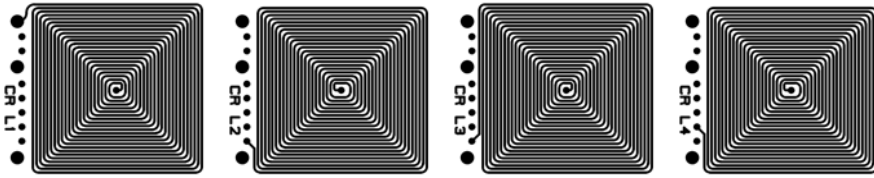
Fig. 8. Individual layers of the multilayer board with buried vias connecting the coils
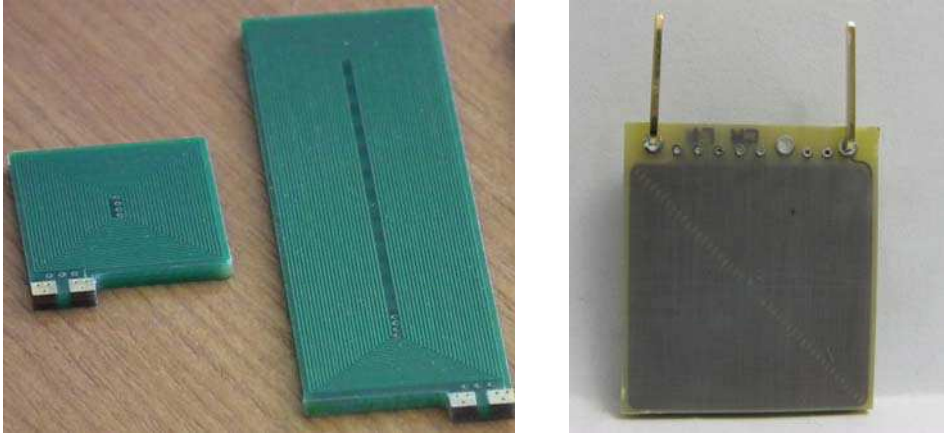

Fig. 9. a) Multilayer boards with through vias, b) multilayer boards with buried vias

The multilayered boards are attached to a base board which provides mechanical support and connects all the boards together electrically. Figure 10 presents some of the base board designs. The base boards are double sided printed circuit boards and their cost is relatively small as compared to the cost of multilayer boards with printed coils on them.

Fig. 10. Various designs of the base board

There are various methods of fastening the multilayered boards to the base board. The one that requires least labor is to squeeze the base boards into the slots milled in the base board as shown in Figure 11 b). Another method uses pins soldered on the one side to the base board and on the other to the multilayer boards, Figure 11 a).
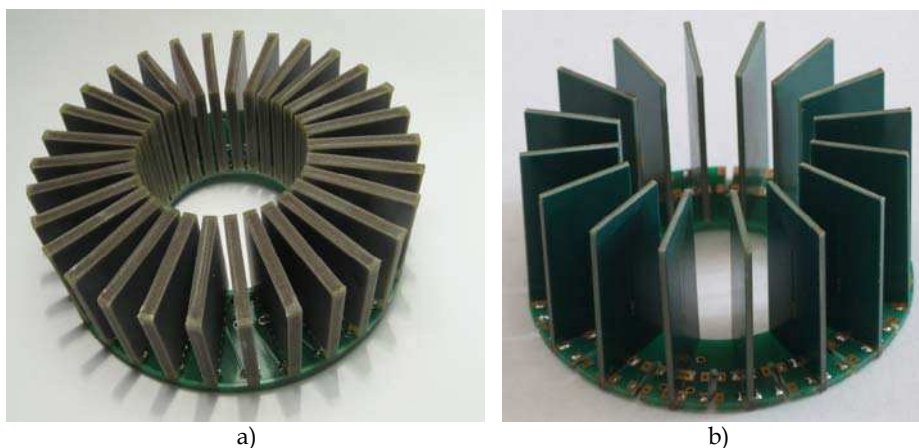

a)   b)

Fig. 11. a) Rogowski coil with pin mounted multilayer boards, b) Rogowski coil with multilayer boards squeezed into the base board

3.2 Design of the coil

The design of the coil starts with the required dimensions of the coil. They determine the dimensions of the multilayer boards and the diameter of the base board. Then it should be determined if the dimensions of the multilayer boards enable to achieve the required coil sensitivity. The minimal thickness of the single layer of the multilayer board is limited by the available technology. Therefore the maximal number of the layers per unit circumference, l_{max}, is fixed. Furthermore, the number of the layers in the multilayer boards is determined by the cost of manufacturing the board. With l bounded by the available technology, the coil sensitivity, according to the equation (5), can only be increased by increasing the A_{ef}. This in turn means thinner tracks and greater coil resistance. It should be said that the coil with higher density of the turns l and lower A_{ef} is superior to the coil with lower l and higher A_{ef}. This is because the sensitivity of the coil to external magnetic fields not connected with the measured current increases with increasing A_{ef}. If the coil dimensions are small, the external magnetic fields are more uniform across the coil. The voltage induced by these fields has equal magnitude but different sign for turns lying on the opposite sides of the coil and the cancellation takes place. The effective area of the spiral inductive coil shown in Figure 12 can be computed with the following formula

$$A_{ef} = \left(\sum_{i=0}^{i=n-1} \left(\left(a - \left(a1 + a2 \right) \right) - \frac{i\left(a - \left(a1 + a2 \right) \right)}{2\left(n \cdot 1 \right)} \right) \left(\left(b - \left(b1 + b2 \right) \right) - \frac{i\left(b - \left(b1 + b2 \right) \right)}{2\left(n \cdot 1 \right)} \right) \right) \qquad (6)$$

where n is the number of the turns in the spiral and a, $a1$, $a2$, b, $b1$ and $b2$ are the dimensions of the mosaic as shown in Figure 12.
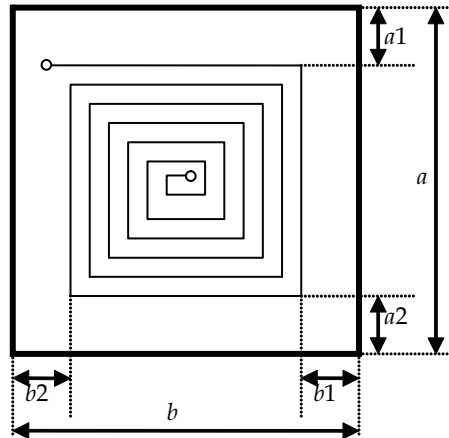
Fig. 12. A simplified printed circuit coil

The upper bound on n in equation (6) is determined by the minimal track thickness. Practical experience shows that the sensitivity of the coil computed using equations (5) and (6) is within 10% of the coil sensitivity obtained from the measurement. The design of the coil is therefore an iterative process. First, given S and l, the value of A_{ef} is computed using equation (5). Then the basic multilayer board is designed using equation (6) and the base board for holding the necessary number of multilayer boards. The coil is manufactured and its sensitivity measured. In the second iteration it is usually necessary to modify only the base board to accommodate slightly smaller or larger number of the multilayer boards.

The PCB technology for Rogowski coils manufacture is characterized by relatively high cost of materials – multilayer PCB are expensive to manufacture, and low cost of man labor. The main advantage of multilayer PCB technology manufacture is that the coils have very repeatable parameters. They can thus be used in applications when exact sensitivity is necessary like in power quality monitoring.

3.3 Voltage transducers

For voltage measurement in wide frequency bandwidth, reactance dividers, resistive dividers and air core transformers can be used. The reactance and resistive dividers have been known for quite a long time and commercial products are available. The resistive dividers, though most accurate of all the transducers provide a galvanic path between the measured primary high voltage and secondary low voltage equipment. The work has been carried out to develop a method to isolate galvanically the resistive divider and preserve at the same time the wide measurement bandwidth. One such solution is an air core transformer.

The voltage transducer made as air core transformer must be characterized by low main inductance which makes it impossible to connect it directly to MV line. In order to limit the current flowing through primary winding it is necessary to use additional elements connected in series with primary winding, Figure 13. These can be resistors or capacitors. The design challenge is to develop an air core transformer with output voltage equal to 200 mV at input current not larger than 1 mA. These conditions result from the necessity to achieve the necessary accuracy (min. 1%) and permissible power dissipation within the

transducer. Because Rogowski coils have no magnetic core, the mutual inductance between individual multilayer boards of the two coils forming the transformer is very low which results in low output voltage. The design objectives that are also not easy to achieve are sufficient isolation between layers and precise and durable boards connection.
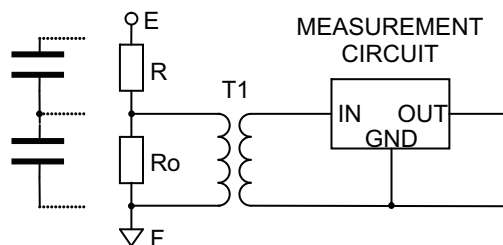

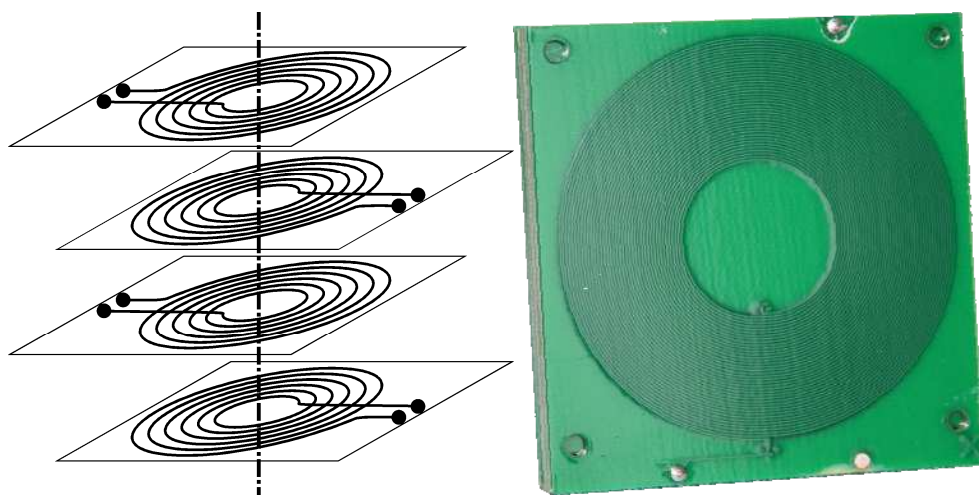Fig. 13. An air core transformer connection in a measurement circuit

Fig. 14. Principle of the air core transformer and its laboratory model

The construction that has been finaly developed at Tele-and Radio Research Institute consists of alternately placed printed circuit boards forming primary and secondary transformer windings respectively. Each board is made up of several layers containing printed coils in the form of spirals. The coils on consecutive layers are conneted in a way preserving the turns directions. The boards are placed with their centers aligned, Figure 14 and as close to each other as possible thus forming a sandwich with two secondary winding boards between every primary winding board.

4. References

Ackerman T. ed. (2005) *Wind Power in Power Systems*, ISBN 0-470-85508-8, John Wiley & Sons, England

Bollen, M. H. J. & Gu I. (2006) *Signal Processing of Power Quality Disturbances*, IEEE Press, ISBN-13 978-0-471-73168-9, USA

European Standard EN 50160: *Voltage characteristics of electricity supplied by public distribution systems*

European Standard EN 61000-4-30:2003: *Electromagnetic compatibility* (EMC) Part 4-30: Testing and measurement techniques – Power quality measurement methods

European Standard EN 61000-4-7:2002: *Electromagnetic compatibility* (EMC) Part 4-7: Testing and measurement techniques – General guide on harmonics and interharmonics measurements and instrumentation, for power supply systems and equipment connected thereto

Gilbert M. (2004) *Renewable and efficient electric power systems*, ISBN 0-471-28060-7, John Wiley & Sons, Inc., Hoboken, New Jersey

http://www.axilane.com/PDF_Files/Rocoil_Pr7o.pdf

Oppenheim A.V. & Schafer R.W. (1998) *Discrete-Time Signal Processing*, 2ed., PH, USA
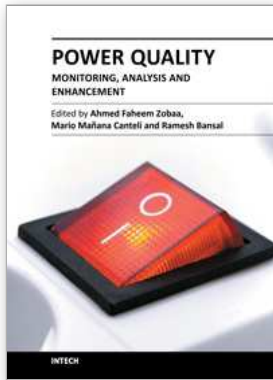
Power Quality â€"Â Monitoring, Analysis and Enhancement

Edited by Dr. Ahmed Zobaa

This book on power quality written by experts from industries and academics from various counties will be of great benefit to professionals, engineers and researchers. This book covers various aspects of power quality monitoring, analysis and power quality enhancement in transmission and distribution systems. Some of the key features of books are as follows: Wavelet and PCA to Power Quality Disturbance Classification applying a RBF Network; Power Quality Monitoring in a System with Distributed and Renewable Energy Sources; Signal Processing Application of Power Quality Monitoring; Pre-processing Tools and Intelligent Techniques for Power Quality Analysis; Single-Point Methods for Location of Distortion, Unbalance, Voltage Fluctuation and Dips Sources in a Power System; S-transform Based Novel Indices for Power Quality Disturbances; Load Balancing in a Three-Phase Network by Reactive Power Compensation; Compensation of Reactive Power and Sag Voltage using Superconducting Magnetic Energy Storage; Optimal Location and Control of Flexible Three Phase Shunt FACTS to Enhance Power Quality in Unbalanced Electrical Network; Performance of Modification of a Three Phase Dynamic Voltage Restorer (DVR) for Voltage Quality Improvement in Distribution System; Voltage Sag Mitigation by Network Reconfiguration; Intelligent Techniques for Power Quality Enhancement in Distribution Systems.

How to reference

In order to correctly reference this scholarly work, feel free to copy and paste the following:

Andrzej Nowakowski, Aleksander Lisowiec and Zdzisław Kołodziejczyk (2011). Power Quality Monitoring in a System with Distributed and Renewable Energy Sources, Power Quality â€"Â Monitoring, Analysis and Enhancement, Dr. Ahmed Zobaa (Ed.), ISBN: 978-953-307-330-9, InTech, Available from: http://www.intechopen.com/books/power-quality-monitoring-analysis-and-enhancement/power-quality-monitoring-in-a-system-with-distributed-and-renewable-energy-sources

INTECH
open science | open minds

www.intechopen.com